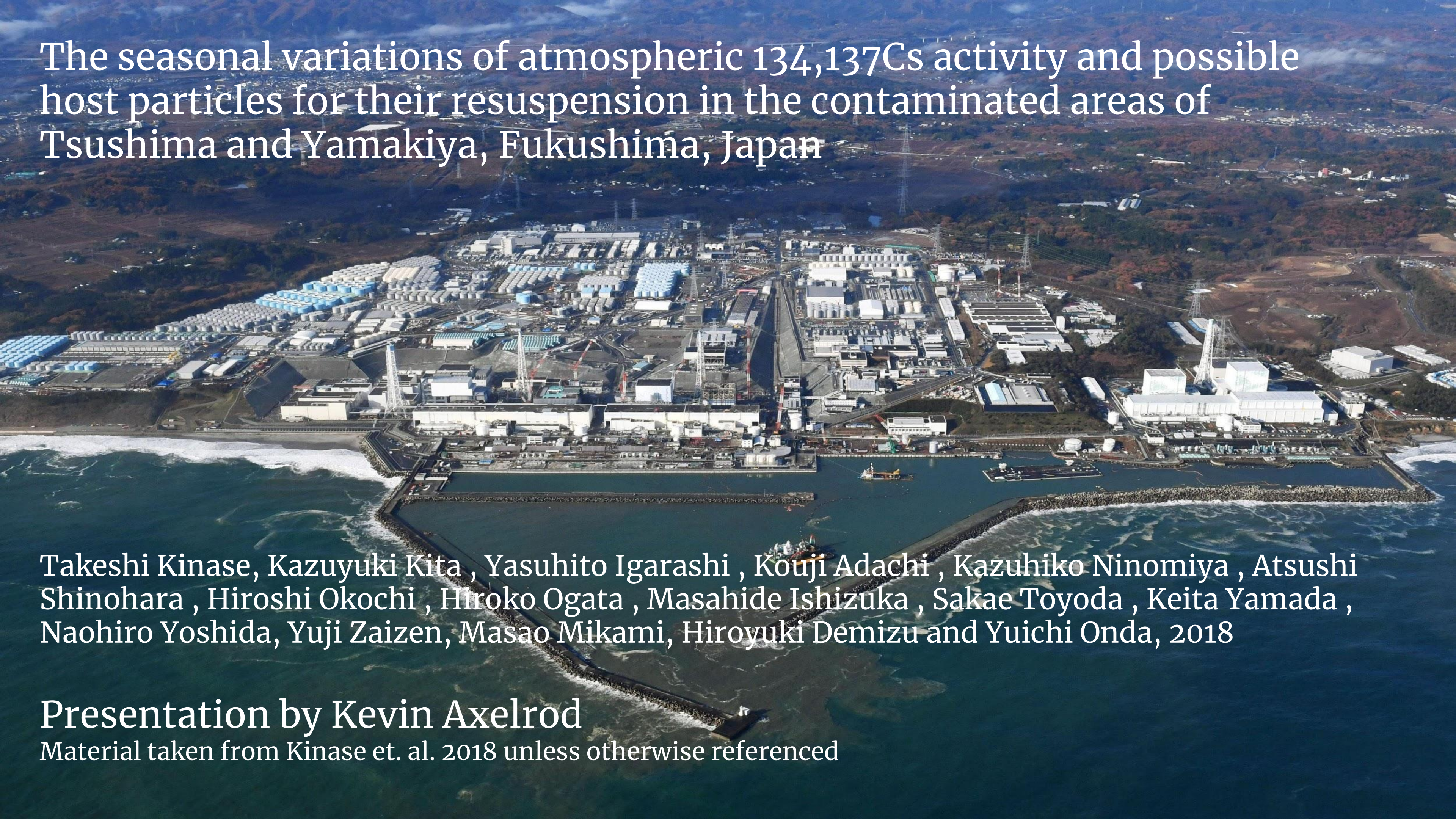

The seasonal variations of atmospheric 134,137Cs activity and possible host particles for their resuspension in the contaminated areas of Tsushima and Yamakiya, Fukushima, Japan

Takeshi Kinase, Kazuyuki Kita , Yasuhito Igarashi , Kouji Adachi , Kazuhiko Ninomiya , Atsushi Shinohara , Hiroshi Okochi , Hiroko Ogata , Masahide Ishizuka , Sakae Toyoda , Keita Yamada , Naohiro Yoshida, Yuji Zaizen, Masao Mikami, Hiroyuki Demizu and Yuichi Onda, 2018

Presentation by Kevin Axelrod

Material taken from Kinase et. al. 2018 unless otherwise referenced

Outline

I. About me
II. Background of the Fukushima-Daiichi nuclear disaster
III. Study by Kinase et al. 2018
    A. Goals of Research
    B. Methods
    C. Results/discussion
    D. Conclusions

IV. References

About me

M.S. student in Atmospheric Sciences

Current research: Bioaerosols

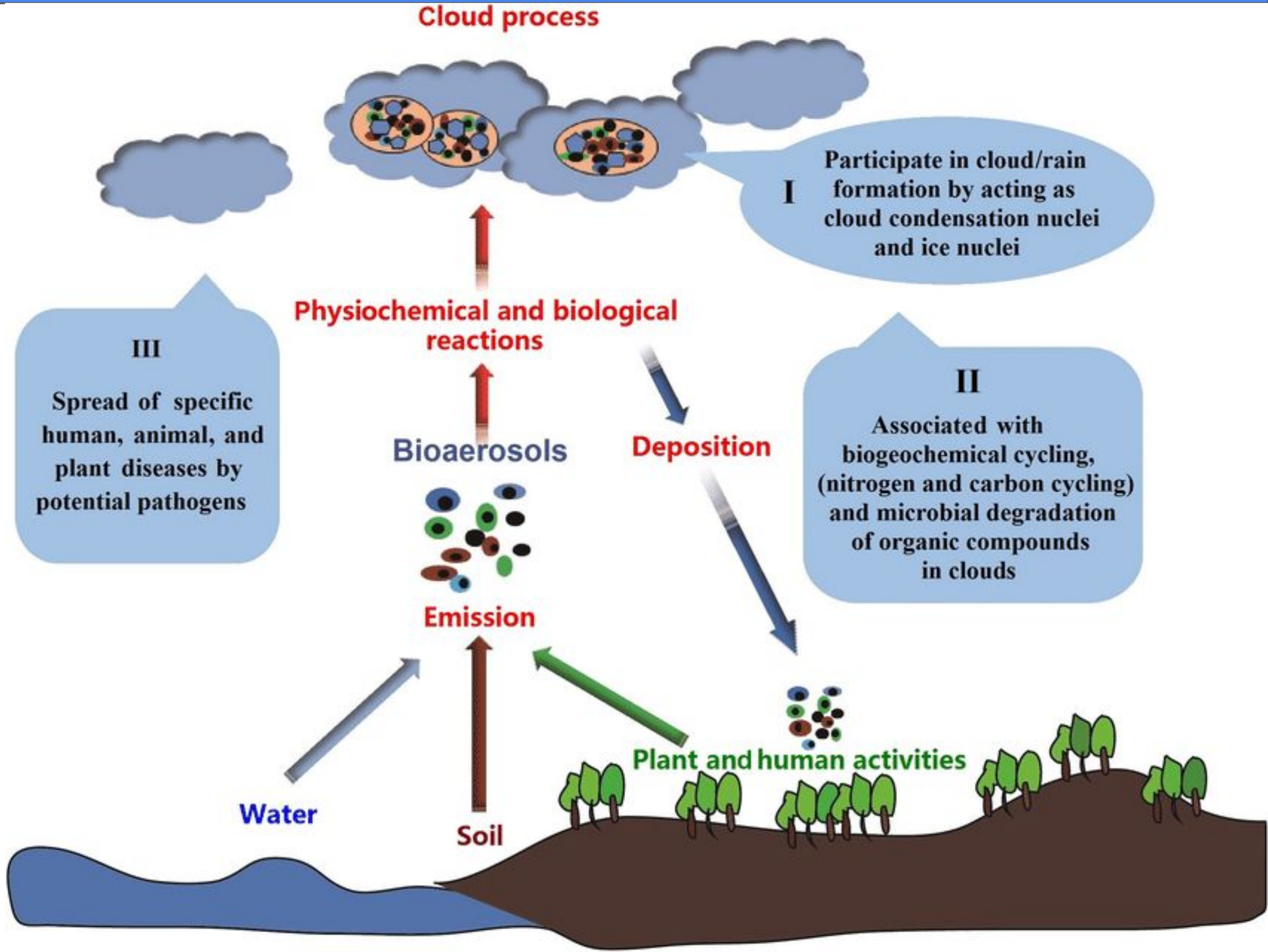

(1)

Background Information

Tohoku Earthquake (The Great East Japan Earthquake of 2011)

Magnitude 9.0-9.1 earthquake occurred off the coast of Japan on March 11, 2011 and resulted in devastating tsunami (highest offshore wave 37.88 m tall)

Total death toll: 18,434 - most of them due to drowning

(3)

(7)

The Fukushima-Daiichi Nuclear accident

Fukushima-Daiichi Nuclear Power Plant was damaged by flooding, and 3 of the plant's 6 reactor cores suffered meltdowns

Radioactive materials released as aerosol: iodine-131, cesium-134, and cesium-137

Focus is on Cesium-134,137 in Kinase et al. 2018

(8)

Evacuation orders given

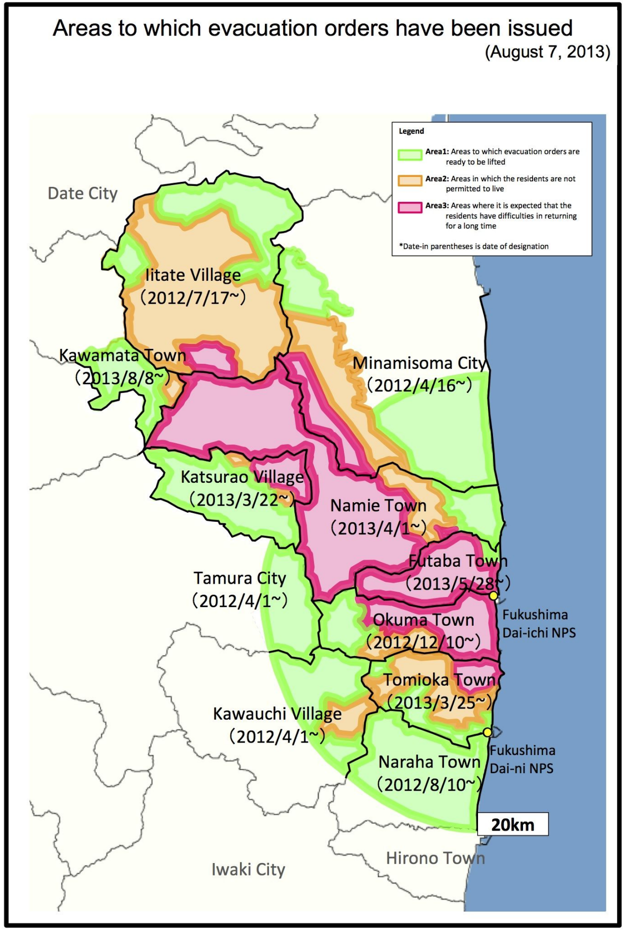

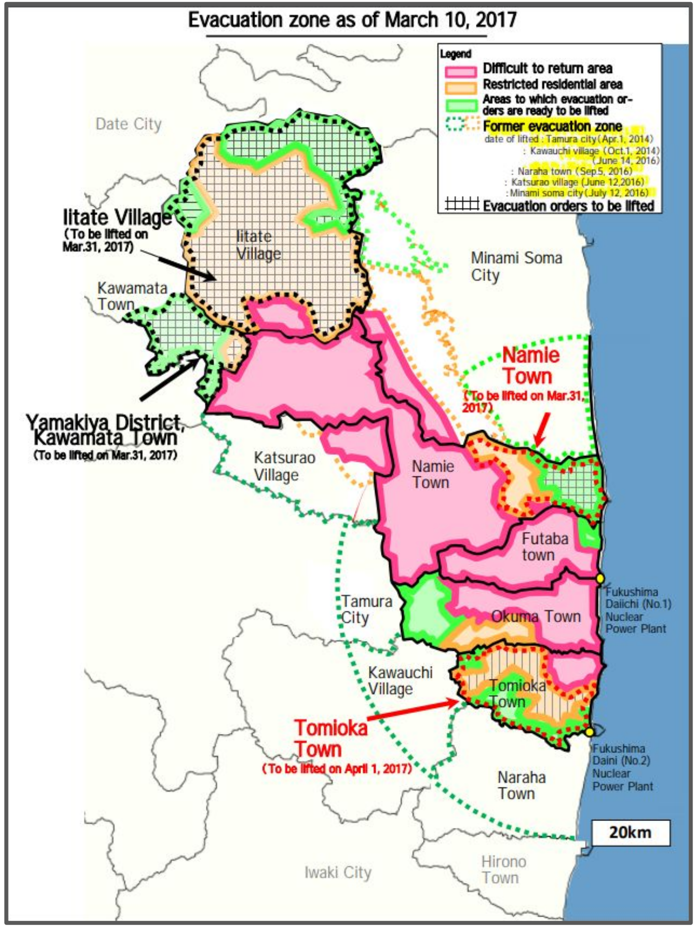

(2)

An overview of radioactive cesium (radiocesium)

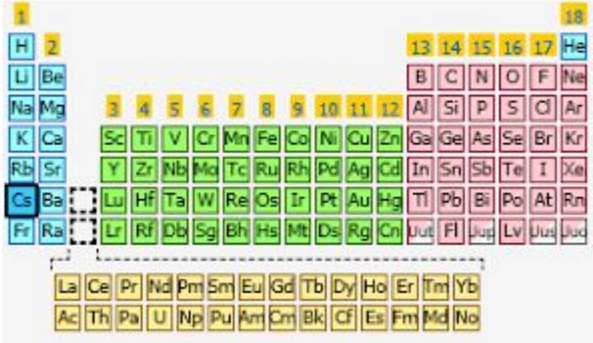

-alkali metal capable of forming salts

-soluble in water

-mimics biological roles of potassium (fluid/electrolyte balance, action potentials)

-both isotopes undergo beta decay and gamma decay

$_{137}$Cs: $\tau_{1/2}$=30.08 years

$_{134}$Cs: $\tau_{1/2}$=2.06 years

(4)

How do we quantify radioactivity?

Bequerel (Bq) - decays per second (units: 1/s) (Kinase et al. 2018 measure in Bq)

Gray (Gy) - a unit of dosage - the amount of radioactive energy absorbed by a person/animal/etc. Used for acute health effects (units: J/kg)

Sievert(Sv) - another unit of dosage - used for stochastic effects like cancer risk (units: J/kg)

Converting a radioactive decay rate into a clear-cut dosage quantity is not an ideal science - many confounding variables, including radiation type, radiation source material, exposure duration, etc. Not an easy job.

How do we quantify radioactivity?

Bequerel (Bq) - decays per second (units: 1/s) (Kinase et al. 2018 measure in Bq)

Gray (Gy) - a unit of dosage - the amount of radioactive energy absorbed by a person/animal/etc. Used for acute health effects (units: J/kg)

Sievert(Sv) - another unit of dosage - used for stochastic effects like cancer risk (units: J/kg)

Converting a radioactive decay rate into a clear-cut dosage quantity is not an ideal science - many confounding variables, including radiation type, radiation source material, exposure duration, etc. Not an easy job.

Kinase et al. 2018

Reason for Kinase et al. 2018

-Examine the prevalence of radiocesium in the Fukushima prefecture by determining patterns and mechanisms of radiocesium aerosol resuspension. Important for determining safety of the area

Resuspension: radiocesium was suspended into atmosphere during the accident, settled, and is now being suspended again by other processes

Reason for Kinase et al. 2018

-Examine the prevalence of radiocesium in the Fukushima prefecture by determining patterns and mechanisms of radiocesium aerosol resuspension. Important for determining safety of the area

Resuspension: radiocesium was suspended into atmosphere during the accident, settled, and is now being suspended again by other processes

Research Goals

1. **Observe and characterize seasonal variations, if any, in atmospheric radiocesium**
2. **Determine spatial scales of resuspension**
3. **Infer as to the host particles responsible for radiocesium resuspension**

Methods: Aerosol sampled in 4 currently or previously contaminated areas in Fukushima

FD: forest, decontaminated

GD: open ground/field, decontaminated

FC: forest, contaminated

GC: open ground/field, contaminated

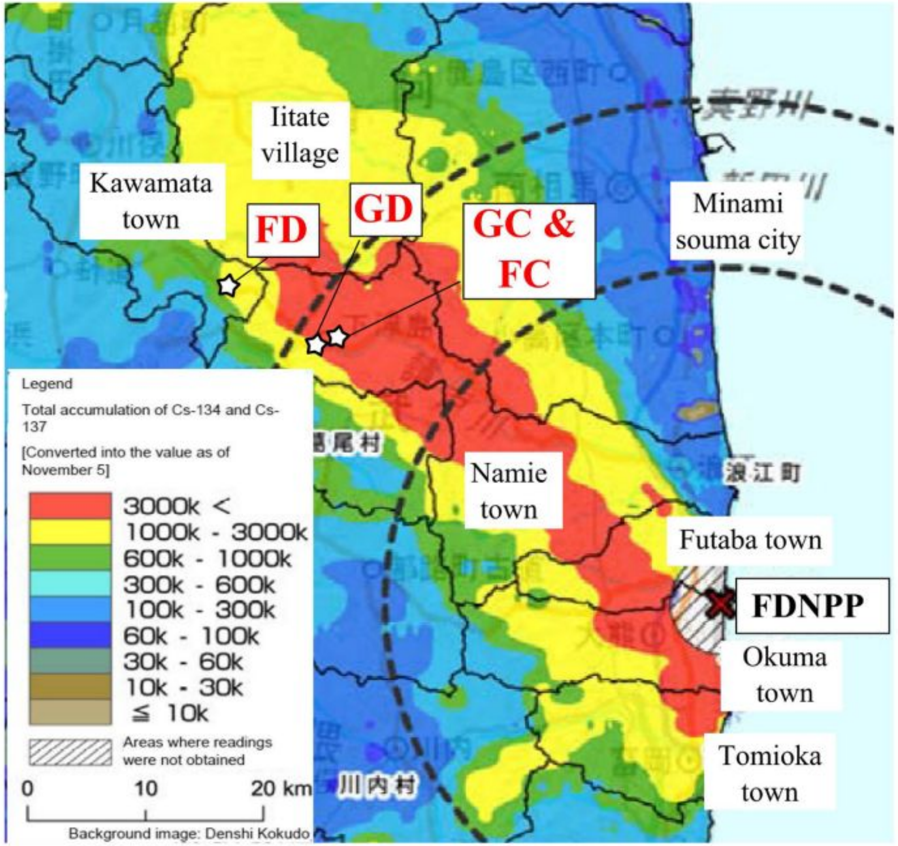

Fig. 1 The four sampling locations in this study plotted over the deposition density map for ^{134,137}Cs obtained by the Japanese government (Ministry of Education, Culture, Sports, Science and Technology, Japan (MEXT) 2011). The radius of dotted outer circle is 30 km

Methods: Sampling techniques and analysis

Aerosol sampling techniques:

-High volume active sampler with quartz filters

-six-stage cascade impactors

(9)

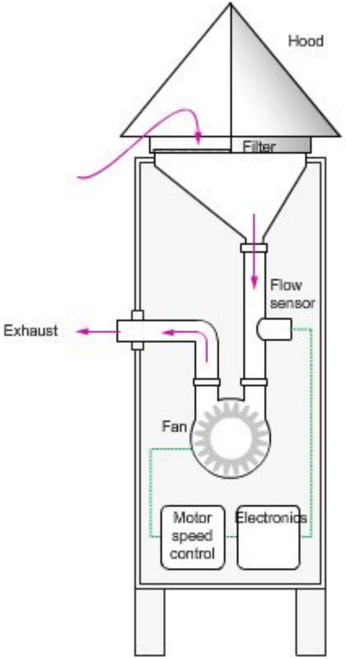

(10)

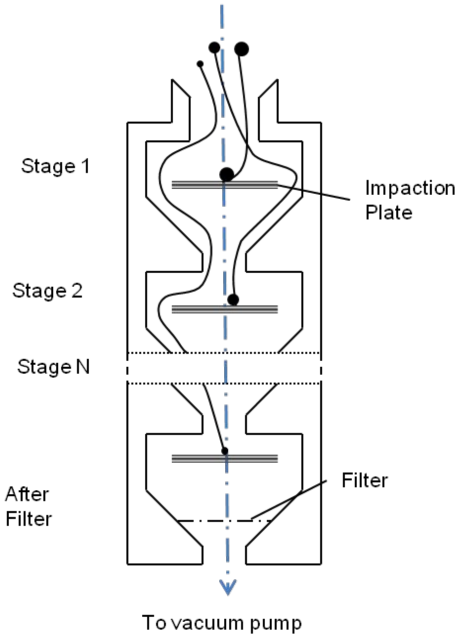

(11)

Using germanium semiconductor detector, radioactivity of 134Cs and 137Cs identified via unique gamma-ray peak intensities at 605 and 662 keV, respectively. Intensities directly related to radioactivity levels.

Radiocesium decay schemes

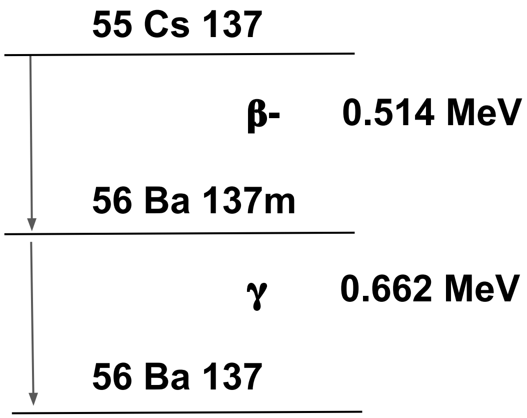

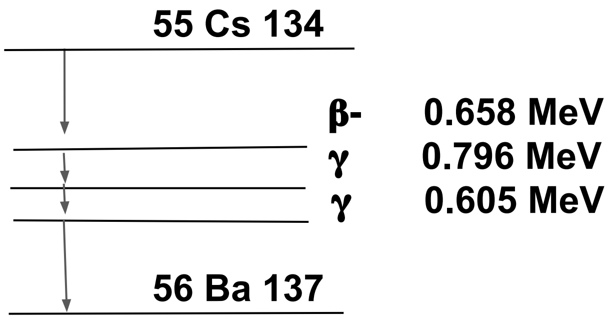

Samples indicated higher atmospheric cesium concentrations in summer

Samples indicate cesium activity:

-peaking in summer months

-dipping down in winter months.

Pattern most evident in GD and GC samples.

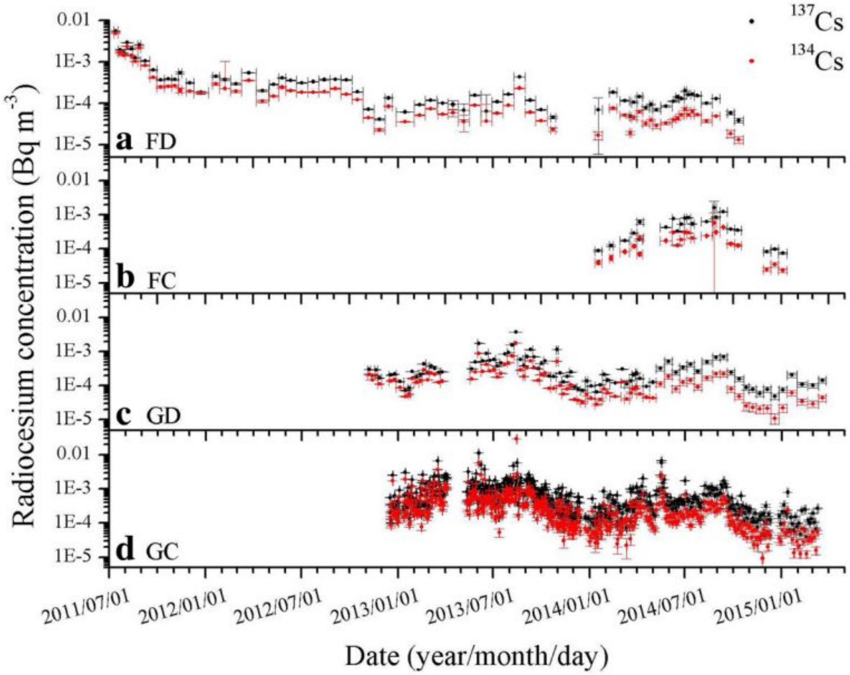

Fig. 2 Activity concentrations of $^{134,137}Cs$ (Bq m^{-3}) measured at the FD, FC, GD, and GC sites in the Fukushima prefecture in July 2011 to March 2015. These results show high concentrations in late spring, summer, and early autumn and low concentrations in winter and early spring at all of the presented observation locations

High-volume samplers' data summary

Table 3 Averages, maximums, and minimums of the ^{137}Cs activity concentration (μBq m^{-3}) at each site

Location (sampling duration)	Average			Maximum				Minimum			
	Year	^{137}Cs	Error	Date (start) m/d h:m	Date (end) m/d h:m	^{137}Cs	Error	Date (start) m/d h:m	Date (end)[a] m/d h:m	^{137}Cs	Error
FD (July 2011–October 2014)	2011	1450	33.7	7/9 16:40	7/18 12:10	5600	66.4	12/9 12:47	2012/1/6 11:16	186	11.0
	2012	287	9.7	3/9 10:43	4/6 11:15	547	7.8	11/16 12:01	12/7 10:18	41.2	2.0
	2013	127	13.6	8/9 14:16	8/30 11:20	432	4.6	10/18 14:48	10/28 10:45	45.9	3.2
	2014	115	8.3	6/29 9:41	7/4 10:30	202	6.4	10/3 10:27	10/20 11:07	38.7	4.6
FC (May 2014–January 2015)	2014	537	78.6	8/22 16:13	8/29 12:52	1620	843	12/26 15:41	2015 1/11 13:24	74.3	5.7
GD (November 2012–June 2015)	2012	213	2.7	11/3 13:40	11/9 12:41	294	2.1	12/28 12:45	2013 1/11 13:46	130	1.4
	2013	521	4.1	8/9 11:55	8/16 11:16	3690	8.0	12/13 12:04	12/23 12:08	72.0	3.0
	2014	243	26.4	9/19 11:16	10/3 10:59	684	94.6	12/26 11:28	2015 1/11 12:07	47.4	8.5
	2015	123	18.7	5/4 11:26	6/4 10:52	225	31.9	4/25 10:41	5/4 11:11	56.8	9.9
GC (December 2012–November 2014)	2012	462	12.2	12/21 13:00	12/22 13:00	2550	28.2	12/19 13:00	12/20 13:00	95.2	4.7
	2013	1170	19.2	8/14 13:00	8/15 13:00	60,400	132	11/12 13:00	11/13 13:00	68.9	11.6
	2014	546	11.6	5/16 13:00	5/18 13:00	6750	31.0	1/15 13:00	1/17 11:38	48.4	7.8

[a]In some cases, the sampling duration crossed over years

High-volume samplers' data summary

Table 3 Averages, maximums, and minimums of the ^{137}Cs activity concentration (μBq m^{-3}) at each site

Location (sampling duration)	Average			Maximum				Minimum			
	Year	^{137}Cs	Error	Date (start) m/d h:m	Date (end) m/d h:m	^{137}Cs	Error	Date (start) m/d h:m	Date (end)[a] m/d h:m	^{137}Cs	Error
FD (July 2011–October 2014)	2011	1450	33.7	7/9 16:40	7/18 12:10	5600	66.4	12/9 12:47	2012/1/6 11:16	186	11.0
	2012	287	9.7	3/9 10:43	4/6 11:15	547	7.8	11/16 12:01	12/7 10:18	41.2	2.0
	2013	127	13.6	8/9 14:16	8/30 11:20	432	4.6	10/18 14:48	10/28 10:45	45.9	3.2
	2014	115	8.3	6/29 9:41	7/4 10:30	202	6.4	10/3 10:27	10/20 11:07	38.7	4.6
FC (May 2014–January 2015)	2014	537	78.6	8/22 16:13	8/29 12:52	1620	843	12/26 15:41	2015 1/11 13:24	74.3	5.7
GD (November 2012–June 2015)	2012	213	2.7	11/3 13:40	11/9 12:41	294	2.1	12/28 12:45	2013 1/11 13:46	130	1.4
	2013	521	4.1	8/9 11:55	8/16 11:16	3690	8.0	12/13 12:04	12/23 12:08	72.0	3.0
	2014	243	26.4	9/19 11:16	10/3 10:59	684	94.6	12/26 11:28	2015 1/11 12:07	47.4	8.5
	2015	123	18.7	5/4 11:26	6/4 10:52	225	31.9	4/25 10:41	5/4 11:11	56.8	9.9
GC (December 2012–November 2014)	2012	462	12.2	12/21 13:00	12/22 13:00	2550	28.2	12/19 13:00	12/20 13:00	95.2	4.7
	2013	1170	19.2	8/14 13:00	8/15 13:00	60,400	132	11/12 13:00	11/13 13:00	68.9	11.6
	2014	546	11.6	5/16 13:00	5/18 13:00	6750	31.0	1/15 13:00	1/17 11:38	48.4	7.8

[a] In some cases, the sampling duration crossed over years

Higher cesium activity: two peaks identified, two inferred causes

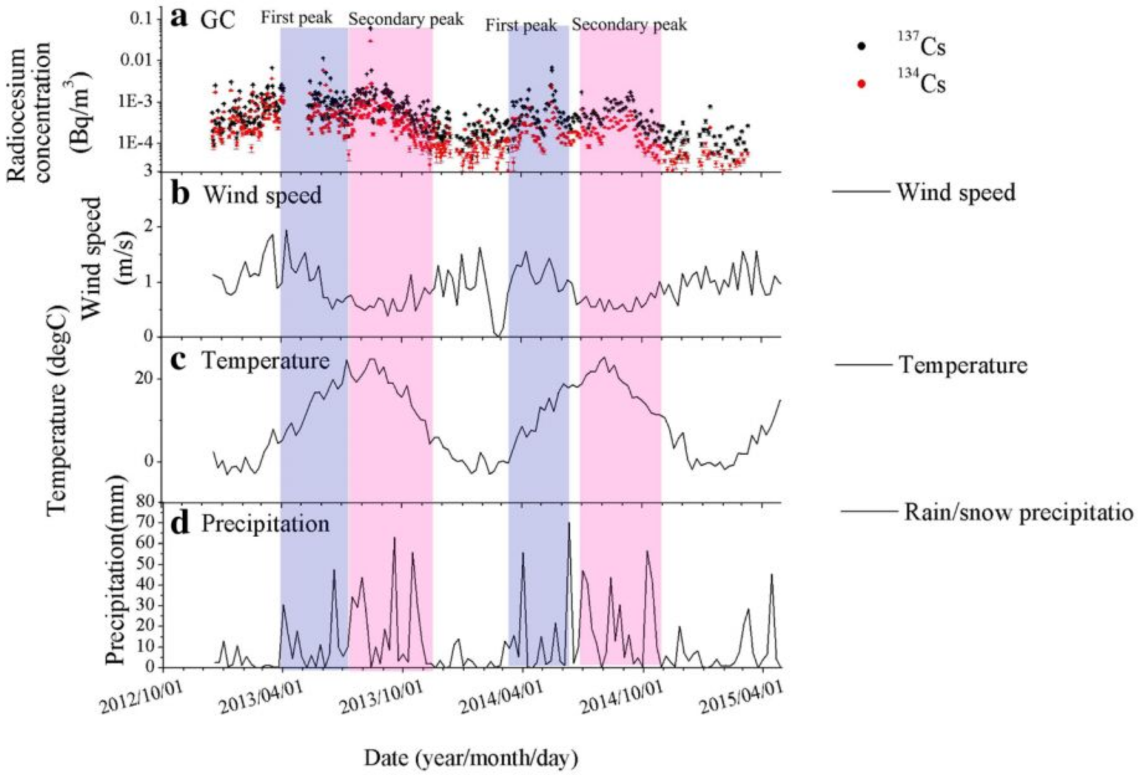

Fig. 3 Time series of (**a**) radiocesium concentrations, (**b**) wind speeds, (**c**) temperatures, and (**d**) rain/snow precipitation. At the GC site, we can see two maxima in the higher concentration seasons: in May and September. The first maxima occurred with wind speed peaks, and the second maxima occurred with atmospheric temperature peaks

Higher cesium activity: two peaks identified, two inferred causes

Peak 1) Seasonal wind speeds increase resuspension of aerosols (type to be identified)

Peak 2) Unclear

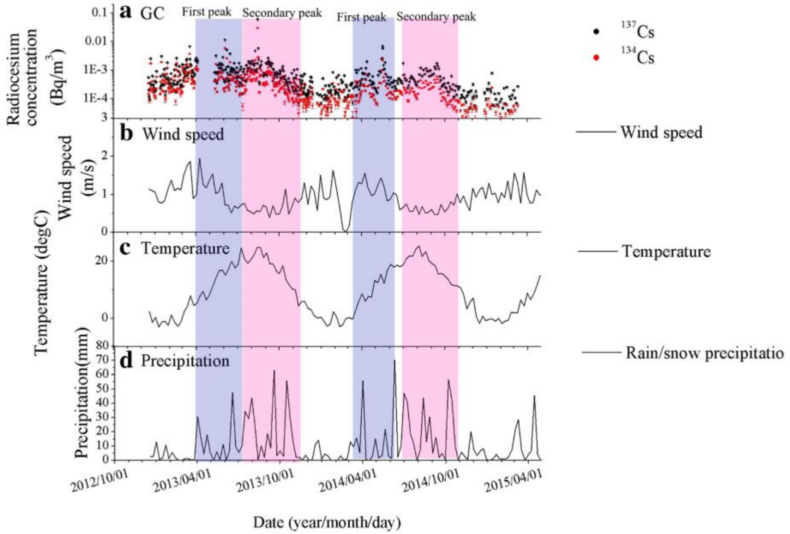

Fig. 3 Time series of (**a**) radiocesium concentrations, (**b**) wind speeds, (**c**) temperatures, and (**d**) rain/snow precipitation. At the GC site, we can see two maxima in the higher concentration seasons: in May and September. The first maxima occurred with wind speed peaks, and the second maxima occurred with atmospheric temperature peaks

Cascade impactor shows seasonal variations in radiocesium

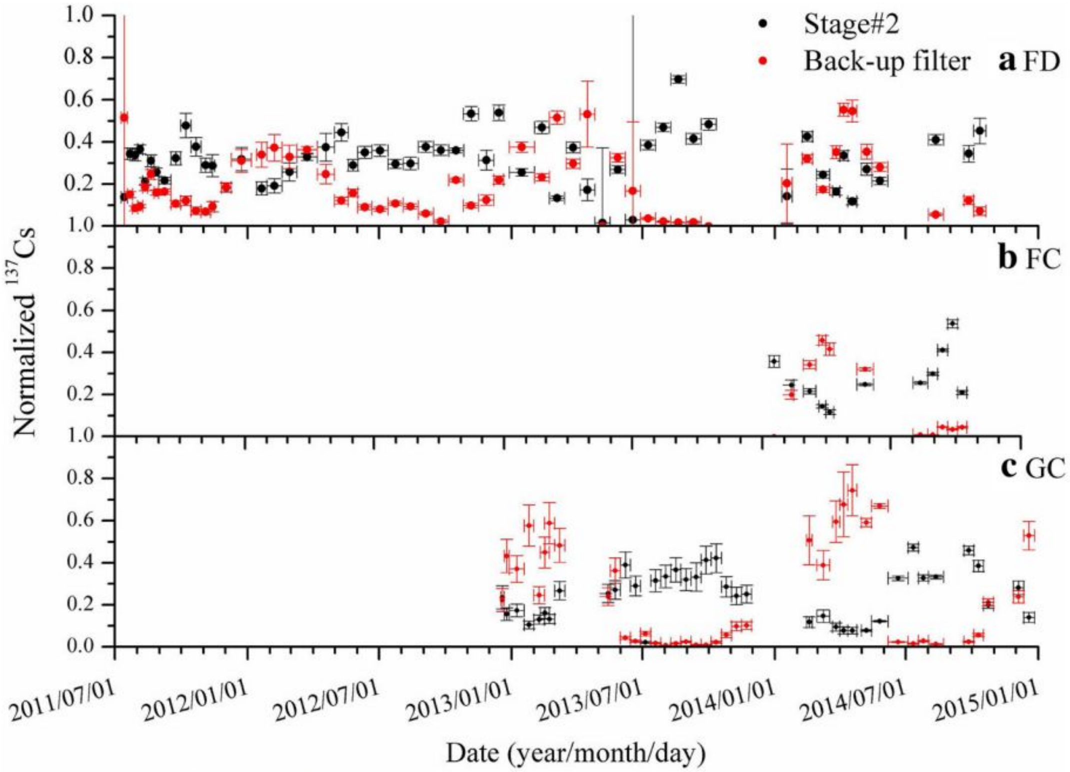

Fig. 4 Time series of the normalized $^{137}Cs_{(2)}$ and $^{137}Cs_{(7)}$ measured at the (**a**) FD, (**b**) FC, and (**c**) GC sites. These results clearly showed the seasonal variation but did not accurately reflect the size distribution of radiocesium in the atmosphere because of the bouncing particles. The amount of bouncing particles significantly changes the collection efficiency of the cascade impactor

Bouncing Particles

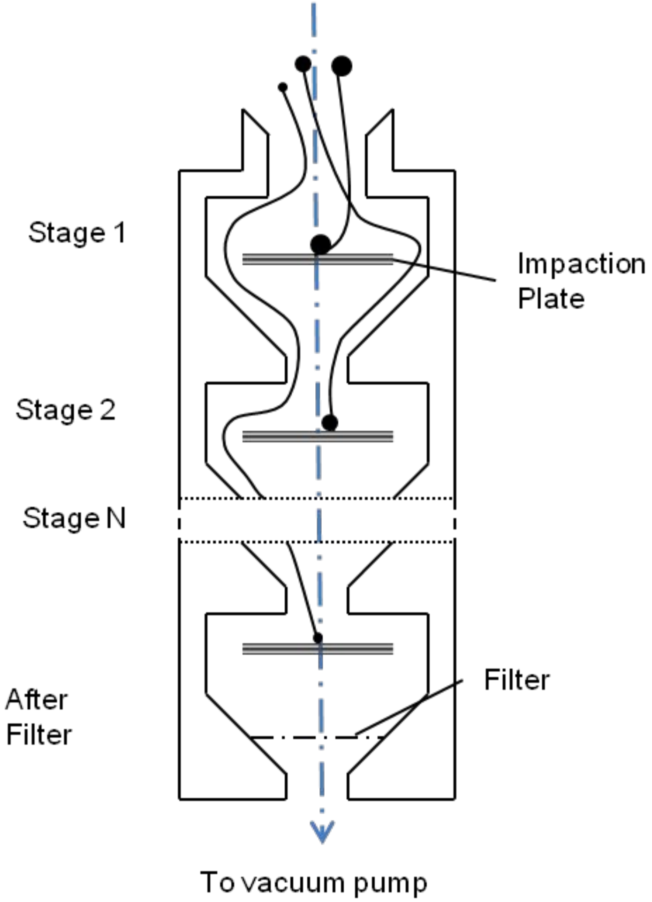

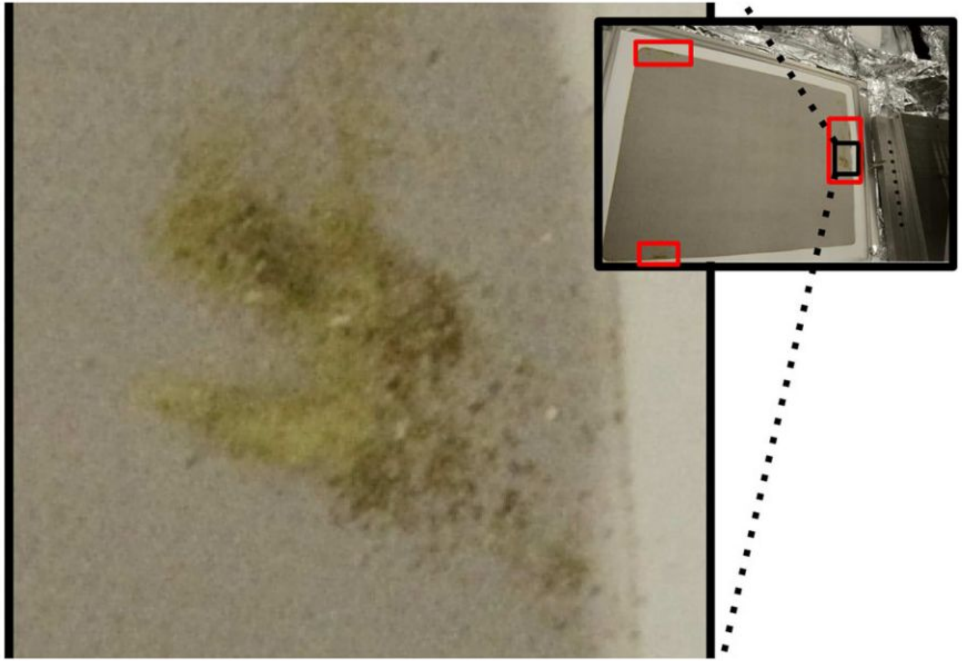

Fig. 5 Picture of a typical backup filter sampled at the GC site in spring (April 2014). We found many coarse particles, which include pollen and coarse soil/mineral dusts, in the areas indicated by the red rectangles

Sampling soil and determining aerosol spatial scale

Coefficient $R_{scale} = {}_{137}Cs_{GD}/{}_{137}Cs_{GC}$

Topsoil measured for radiocesium activity at 2 sites:

GD: 2.17 ± 0.07 Bq/g

GC: 128 ± 3.9 Bq/g

Soil R_{scale} = .017

Aerosol R_{scale}: Fig. 7

Higher-than-expected R_{scale} indicate spatial scale of local atmospheric Cs transport may extend from contaminated zones into decontaminated zones.

Seasonal variations also apparent in both R_{scale} and particle bounce.

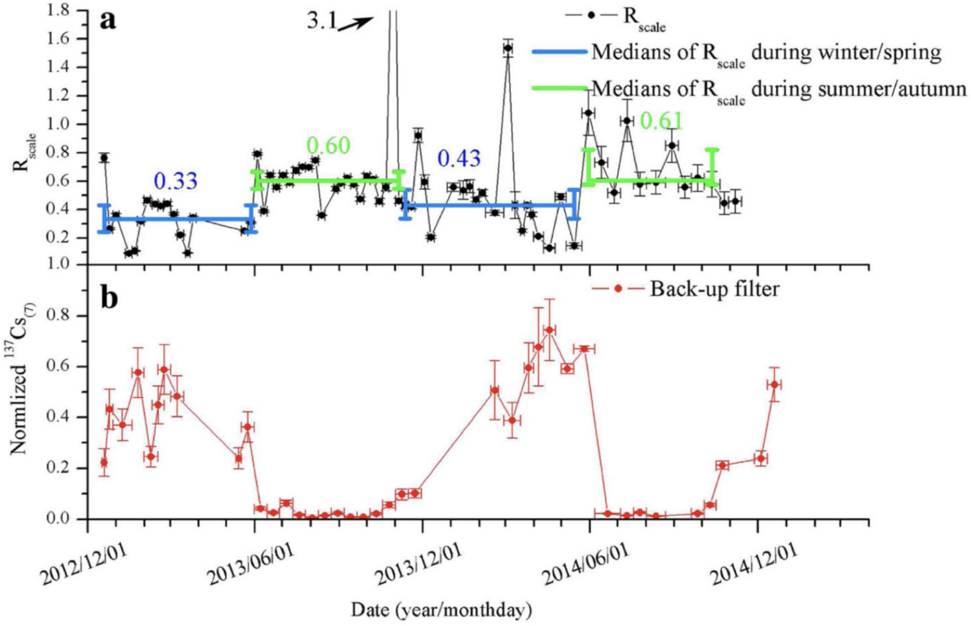

Fig. 7 Time series of **a** R_{scale} and **b** normalized $^{137}Cs_{(7)}$ at the GC site and **c** the correlation plot of R_{scale} and the normalized $^{137}Cs_{(7)}$. Green and blue curves in **a** are the medians of R_{scale} in summer/autumn and winter/spring, respectively. The error bars for each curve in **a** and **b** show the range of central 50%

Investigation of the effects of biomass burning on atmospheric radiocesium concentrations

Levoglucosan: organic tracer compound known to be a product of biomass burning

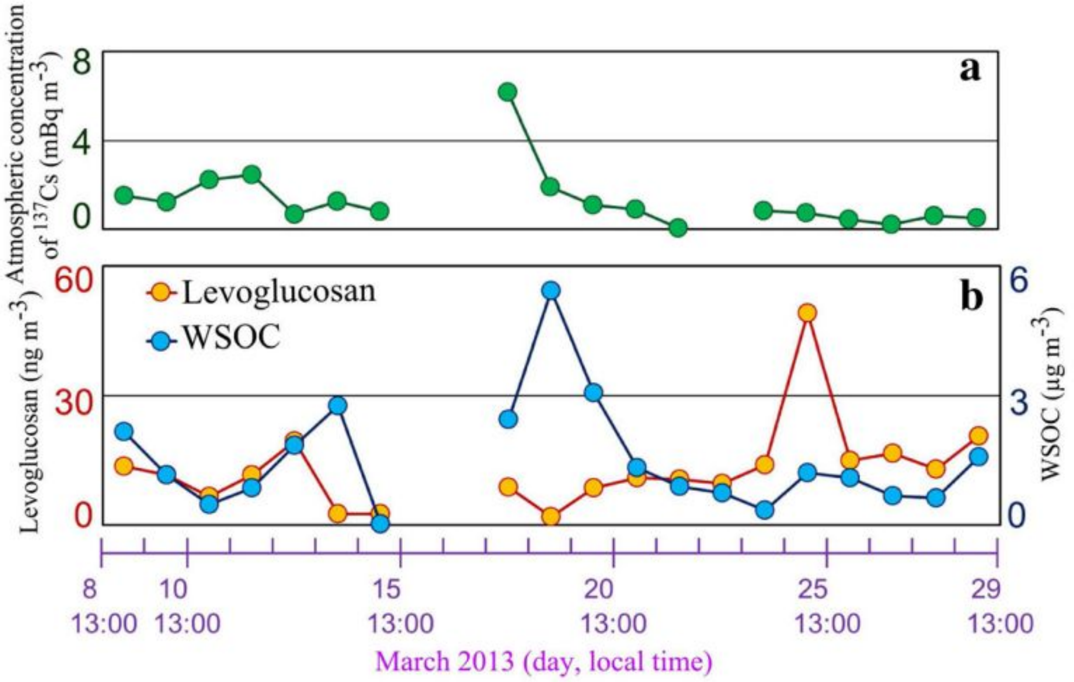

Fig. 8 Time series of **a** the radiocesium concentrations and **b** the concentrations of levoglucosan and WSOC in the atmosphere at GC

Investigation of the effects of biomass burning on atmospheric radiocesium concentrations

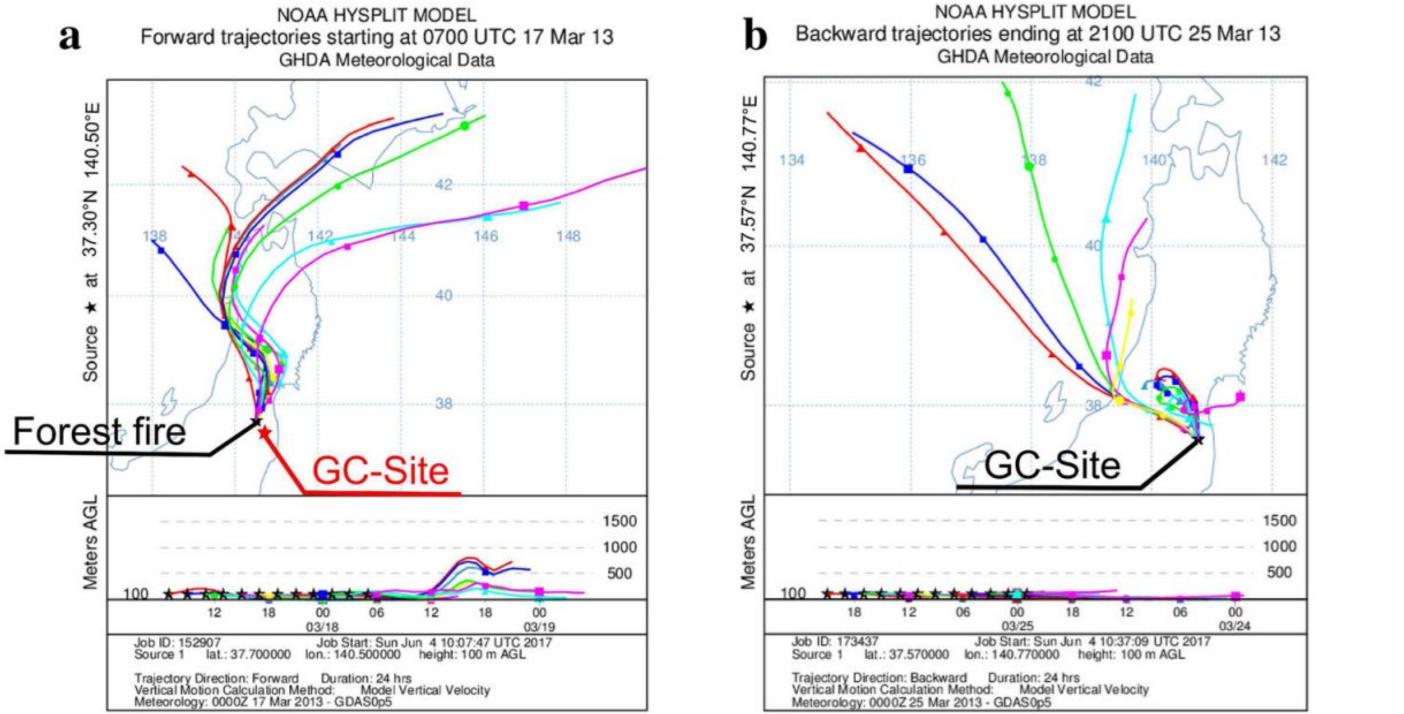

Fig. 9 Maps show the forward and backward trajectories calculated with NOAA HYSPLIT model (Stein et al. 2015) during the forest fire event. **a** The forward trajectories from Ootaki (forest fire area), which are calculated from March 17 at 16:00 (LT) to March 18 at 13:00 (LT). **b** Backward trajectories from the measurement site (GC), which are calculated from March 24 at 13:00 (LT) to March 25 at 13:00 (LT)

Investigation of bioaerosols: Sampling filters analyzed under SEM

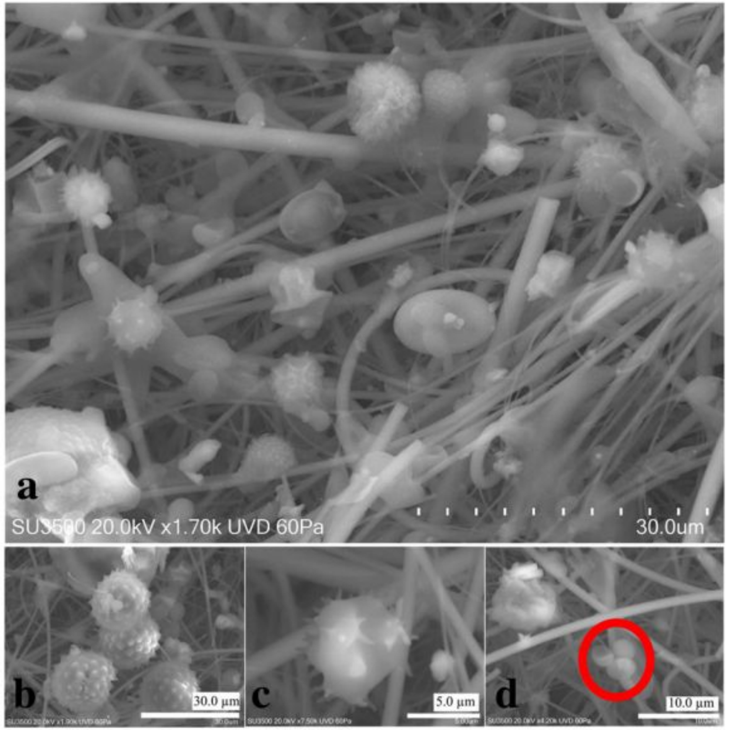

Fig. 11 Examples of organic particles in the samples obtained in September 2014 at the GD site. **a** A SEM image of the wide visible range. **b** Pollen. **c** Spore. **d** Microorganisms (surrounded by red circles)

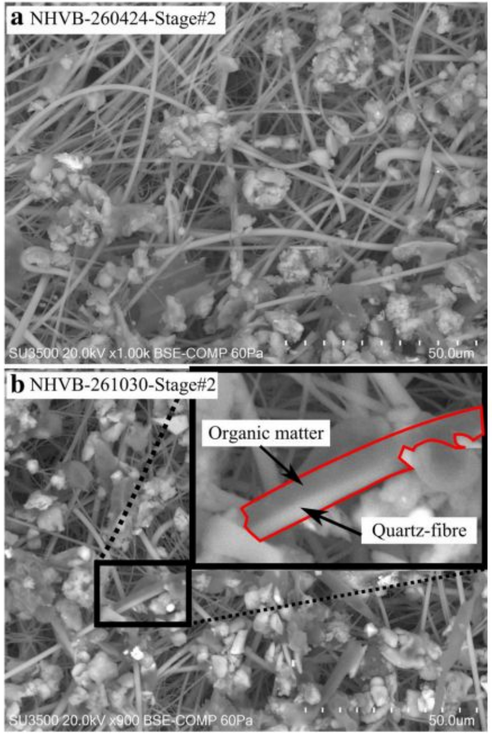

Fig. 6 SEM images of filters for stage #2 sampling at the GC site in **a** spring and **b** autumn. The adhesive organic matter that sticks to the quartz fiber is surrounded by the red line. From the morphology, we suspect that the material was dense liquid when it was suspended in air. This matter probably affects the collection efficiency of the coarse particles on the filter

Bioaerosol counts

137-Cs concentrations significantly higher in summertime samples, correlating with bioaerosol concentrations

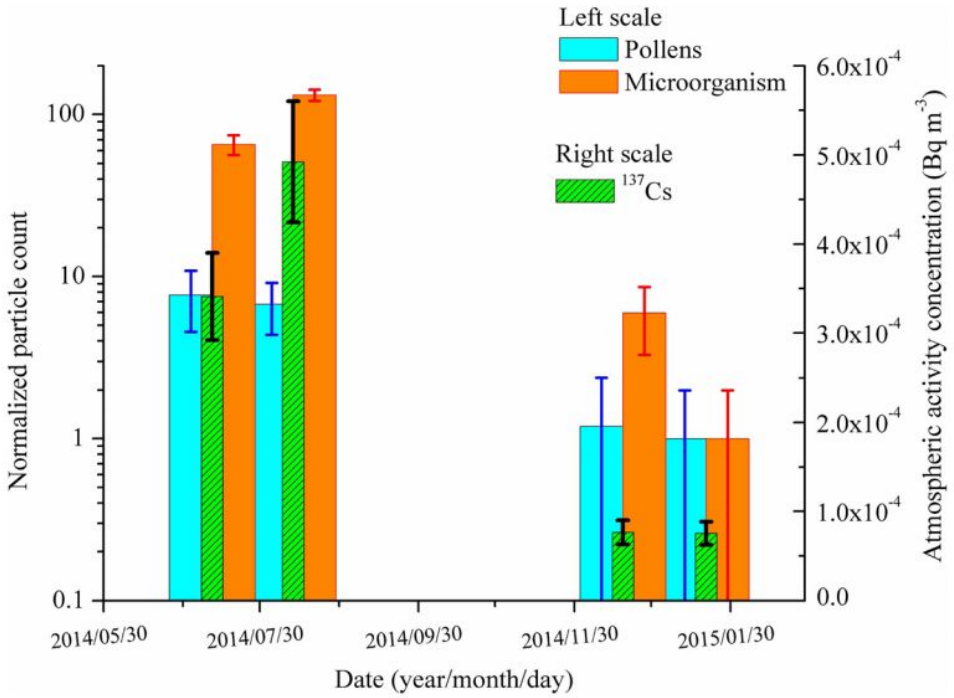

Fig. 12 The normalized particle count of the bioaerosols using SEM (in relative values, the error bar shows the Poisson standard deviation) and atmospheric concentrations of ^{137}Cs activity sampled at the GD site during summer (July and August 2014) and winter (December 2014 and January 2015). The counts of microorganisms include those of spores (see the text)

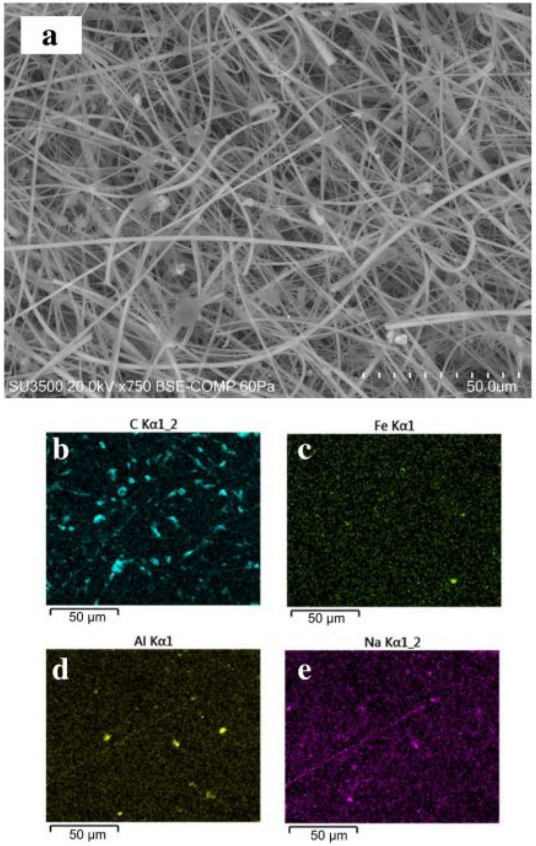

Fig. 10 The SEM image and elemental mapping images of the sample filters obtained at the GD site in July 2015. **a** The SEM image, (**b**) the elemental map of C, (**c**) the elemental map of Fe, (**d**) the elemental map of Al, and (**e**) the elemental map of Na. The characteristic organic particles commonly exist in the filter samples

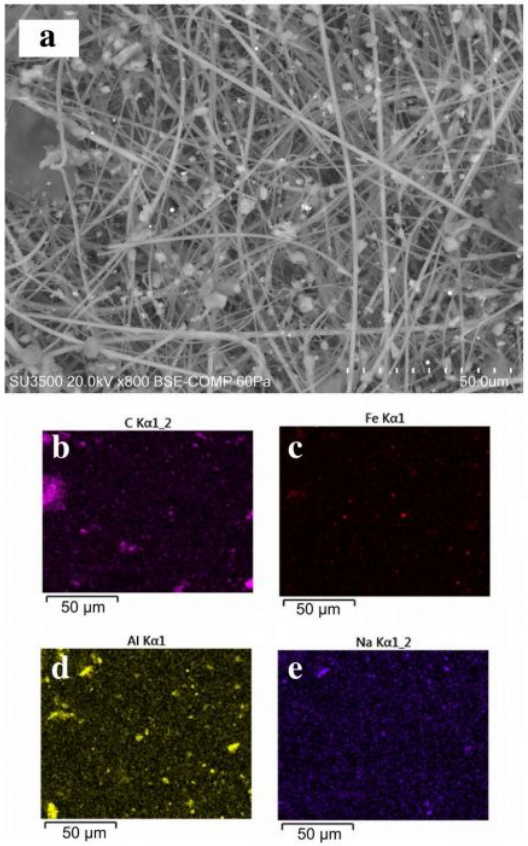

Fig. 13 The SEM and elemental mapping images of the sample filter obtained at the GD site in January 2015. **a** The SEM image, (**b**) the elemental map of C, (**c**) the elemental map of Fe, (**d**) the elemental map of Al, and (**e**) the elemental map of Na. Major coarse particles include Al (clay mineral) and Na (salt or mineral)

Why bioaerosols could be the culprit of high summertime Cs

-Many bioaerosols are seasonal and occur in warmer months of the year

-Bioaerosol emitters may selectively absorb cesium for its biological functions

Conclusions

-observed seasonal variations in atmospheric radiocesium concentrations in rural Fukushima

-soil/mineral dust and debris are the most abundant types of aerosol in winter and spring

-biomass burning not implicated in high atmospheric Cs concentrations

-bioaerosols correlated with high atmospheric Cs in summer and fall, although a quantitative relationship was not determined and specific bioaerosols were not identified

Bigger picture: does this even matter?

While levels of radioactivity in many parts of Fukushima are still orders of magnitude greater than background radiation, it is unclear how/if they pose a danger to humans due to the lack of knowledge/research in long-term radiation exposure.

Bigger picture: does this even matter?

While levels of radioactivity in many parts of Fukushima are still orders of magnitude greater than background radiation, it is unclear how/if they pose a danger to humans due to the lack of knowledge/research in long-term radiation exposure.

References

1. Min Wei et al. “Characteristics of bacterial community in cloud water at Mt Tai: similarity and disparity under polluted and non-polluted cloud episodes.” *European Geosciences Union.* Atmos. Chem. Phys., 17, 5253–5270, 2017. Print. doi:10.5194/acp-17-5253-2017. https://www.researchgate.net/publication/316439607_Characteristics_of_bacterial_community_in_cloud_water_at_Mt_Tai_Similarity_and_disparity_under_polluted_and_non-polluted_cloud_episodes
2. “Evacuation Orders and Restricted Areas.” *Fukushima on the Globe*, 31 Mar. 2017, fukushimaontheglobe.com/the-earthquake-and-the-nuclear-accident/evacuation-orders-and-restricted-areas. http://fukushimaontheglobe.com/the-earthquake-and-the-nuclear-accident/evacuation-orders-and-restricted-areas
3. Dunbar, Paula. *National Centers for Environmental Information*, National Oceanographic and Atmospheric Administration, www.ngdc.noaa.gov/nndc/struts/results?EQ_0=5413&t=101650&s=9&d=101%2C91%2C95%2C93&nd=display.
4. Gagnon, Steve. “It's Elemental - Isotopes of the Element Cesium.” *Thomas Jefferson National Accelerator Facility - Office of Science Education*, education.jlab.org/itselemental/iso055.html.
5. “55 Cs 137.” *Nucleonica*, www.nucleonica.com/Application/ReducedDecaySchemes/Cs137_TXT.htm.
6. “55 Cs 134.” *Nucleonica*, www.nucleonica.com/Application/ReducedDecaySchemes/Cs134_TXT.htm.
7. Vogt, Gregory L. “Japanese Earthquake and Tsunamis: Before and After.” *BioEd Online*, Baylor College of Medicine, 11 Feb. 2013, www.bioedonline.org/news/hot-topics/japanese-earthquake-and-tsunamis-before-and-after/.
8. Rafferty, John P. *Fukushima Accident*. Encyclopædia Britannica, Inc., 13 Mar. 2018, www.britannica.com/event/Fukushima-accident.
9. Photo courtesy of K Balakrishna, https://slideplayer.com/slide/13602132/
10. Diagram courtesy of Queensland Government, https://www.qld.gov.au/environment/pollution/monitoring/air/air-monitoring/measuring/samplers
11. Diagram courtesy of Wikipedia, https://en.wikipedia.org/wiki/Cascade_impactor